Model Evaluation for Computer Graphics Renderings of Artist Paint Surfaces

Ying Chen, Roy S. Berns, Lawrence A. Taplin; Munsell Color Science Laboratory, Chester F. Carlson Center for Imaging Science; Rochester Institute of Technology, Rochester, New York, USA

Abstract
Light reflection models for computer graphics have been developed over the past several decades. For real paint surfaces, it is possible to model their bidirectional reflectance distribution function with simple models. This research established a framework to evaluate two simple reflection models, Phong and Torrance-Sparrow, which were used to render artist paint surfaces under different illumination angles. An image acquisition system was set up to capture the images under selected illuminated angles. The parameters of the specular and the diffuse components were estimated with these image sequences. At the evaluation stage, both physical-based metrics and psychophysical techniques were used to evaluate the estimation accuracy of each model. For both methods, the comparison of the estimations of two models showed that better estimations were obtained from the Torrance-Sparrow model for the glossy samples. The estimation accuracies of two models are almost the same for the matte samples. In addition, the numbers of illumination angles of the test samples can be minimized based on both mathematical calculations and psychophysical experiments.

Introduction
For realistic scenes, the spectral and geometric properties of the light source, object, and observer determine appearance. Thus, the interplay of the lighting, viewing and object properties must be considered in the digital reproduction of objects in display and print. Commonly, the photographer defines a specific set of geometric conditions, reducing the myriad geometric experience to a single representation. Alternatively, if data are available as a function of this interplay, known as the bidirectional reflectance distribution function (BRDF),[1] images can be rendered for a variety of geometries and in combination, simulate the real-time viewing experience.

A variety of reflection models have been proposed to calculate BRDF, including both physical-based and empirical models. The Phong[2] and Ward[3] models are two common empirical models, which were derived from measured data. Blinn[4] introduced the Torrance-Sparrow[5] physical-based light reflection model to computer graphics, and replaced the standard Gaussian distribution with ellipsoids of revolution[6] in modeling microfacets. Over the past several decades, more physical-based models were proposed with more optical and physical properties and more complex distribution of microfacets. In addition, Dana[7] defined bidirectional texture function (BTF) to describe the function of the texture surfaces. One difficulty of the measurement system is that the camera position must be calibrated accurately since the camera was moved to different locations. Malzbender[8] in HP Labs presented polynomial texture mapping to reconstruct the luminance of each pixel. However, the specular component was not directly modeled and must be handled separately.

Although there are many studies on BRDF and BTF measurement and 3D image rendering, research focusing on artist paint surfaces are limited. Hawkins[9] proposed an approach to render cultural artifacts based on capturing the reflectance fields of the objects, but a large amount of images are required. Tominaga[10] also proposed a method to record and render art paintings. However, only a matte oil painting was tested in his research. The purpose of this research was to develop a practical apparatus for the museum to record 2D artist paint surfaces under different illumination angles, and then render them with different light reflection models and evaluate their accuracy. Because of their mathematical simplicity and small number of parameters, Phong and Torrance-Sparrow models were selected from the empirical and physical-based models to estimate the specular and diffuse components. Eight different paint samples with different gloss levels were selected to evaluate the models. The performance of the models were evaluated and compared for both physical-based and psychophysical methods. Furthermore, the numbers of the lighting geometries needed to fit the model can be minimized for different measured samples.

Image-based Acquisition System

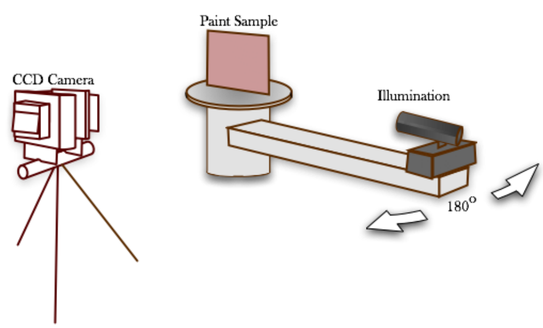

***Figure 1**. Image sequence acquisition system*

The image sequence acquisition system is shown as Figure 1. The Mille Luce fiber optic illumination made by StockerYale was used for illumination. Currently, the system has one degree of freedom of illumination position, which can be changed by moving the lighting arm. Thus, only a series of polar illumination angles changed with the constant azimuth illumination angle.

In the viewing position, a Nikon D1 CCD camera was fixed. To estimate the parameters in the BRDF models, the relative radiance of each pixel should be known. Thus, the opto-electronic conversion functions (OECF) of three channels of the camera were measured and calculated according to ISO 14524.[11] In order to capture the image with 0° illumination angle, there is a small angle between the optical axis of the camera and sample normal.

Lighting Reflection Models

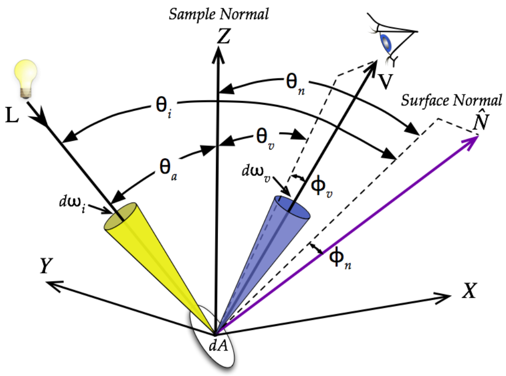

***Figure 2**. Light reflection geometry in terms of illumination and viewing angles and surface tilt angles*

Figure 2 depicts the light reflection geometry of the complex paint sample surface. Two normal directions are shown in the figure, the sample normal Z and the surface normal N of an element dA. The incident and view directions are specified by θ_i and (θ_v, ϕ_v), respectively. The element surface normal in terms of the sample normal is represented by two tilt angels, θ_n and ϕ_n. The illumination angle θ_a of the sample surface can be obtained and this angle changes only in the XZ plane. All the angles are defined as either positive or negative angles, since the same angles might exist on two sides of the Z-axis. The angles defined in this reflection geometry are different with that in traditional BRDF specification. The purpose of this definition is to simplify the mathematical calculation.

Phong Model

The Phong[2] model controls four parameters to determine the gonio-radiometric values. Thus, the relative radiance in the Phong model is expressed as the function of the above angles depicted in Figure 2, shown in Eq. (1).

$$\begin{aligned} &Y = Ae + Ad\cos\theta_i + As(\cos\theta_s)^n \\ &\cos\theta_i = \cos(\theta_a - \theta_n)\cos(\phi_n) \\ &\cos\theta_s = \cos\phi_v \cos\phi_r \cos(\theta_v - \theta_r) + \sin\phi_v \sin\phi_r \\ &\sin\phi_r = \sin(2\phi_n)\cos(\theta_a - \theta_n) \end{aligned} \tag{1}$$

where Ae, Ad and As are the magnitude parameters of the ambient, diffuse and specular components; ϕ_r is the angle between the plane XZ and the perfect mirror reflection direction; θ_r is the angle between the sample normal and the projection of perfect mirror reflection on XZ plane; θ_s is the angle between the view angle and the perfect mirror reflection direction of the incident light; n describes the measured shininess of the surface.

Torrance-Sparrow Model

Based on geometrical optics, Torrance and Sparrow[5] derived a theoretical model for roughened surfaces. In this model, the surface element was assumed to consist of small randomly dispersed mirror-like facets. This model can be described as Eq. (2).

$$\begin{aligned} &Y = Ad\cos\theta_i + As\left(\frac{DGF}{\cos\theta_{vn}}\right) \\ &\cos\theta_i = \cos(\theta_a - \theta_n)\cos\phi_n \\ &\cos\theta_{vn} = \cos\phi_n \cos\phi_v \cos(\theta_v - \theta_n) + \sin\phi_n \sin\phi_v \end{aligned} \tag{2}$$

where D is the standard Gaussian distribution function of the direction of the microfacets and F is the Fresnel reflection, which is the function of θ_i and refraction index n. In this research, the n value of the resin, 1.5, was used. G is defined as the geometrical attenuation factor and represents the remaining light amount after the shadowing and masking, which is a function of θ_a, θ_n, ϕ_n, θ_v and ϕ_v.

Another facet distribution function that models the microfacets as ellipsoids of revolution, proposed by Trowbridge and Reitz,[6] provided a better match to the experimental data than that in Torrance-Sparrow model. In order to improve the computation results, this facet distribution function was used in this research, shown in Eq. (3).

$$D = \left[\frac{c^2}{(\cos\theta_{\hat{N}\hat{H}})^2(c^2-1)+1}\right]^2 \tag{3}$$

where c is the eccentricity of the ellipsoids; $\theta_{\hat{N}\hat{H}}$ is the angle between the surface normal H and the bisector vector of incident and view vectors.

Estimation of Model Parameters

With the image sequence under different illumination angles, the parameters in the models can be estimated according to the flow chart, illustrated in Figure 3. All the calculations were performed in MATLAB. Based on the Phong and Torrance-Sparrow models, the diffuse and specular components should be separated before the estimation of the parameters. One simple way to do this is to suppose that there is no specular component for the large illumination angles. Thus, it is very easy to set up a threshold of illumination angle for one kind of material, which can be used to determine the diffuse component. The separation result of a paint sample is shown in Figure 4. The threshold of this sample is ±35° from the highlight peak angle.

Parameters Estimation for Diffuse Component

As described in Eqs. (1) and (2), the diffuse component of the model only depends on the incident angle and surface normal. Thus, the surface orientation could be estimated from the diffuse component. There are five parameters in the Torrance-Sparrow model and six in the Phong model that need to be estimated for each pixel. The data were nonlinearly fitted with the 'nlinfit' function, in which the Gauss-Newton method is used. Three estimated diffuse magnitude values of three primaries determine the color of the pixel. Since illumination angle in the system changes only in XZ plane, θ_n and the absolute value of ϕ_n can be obtained.

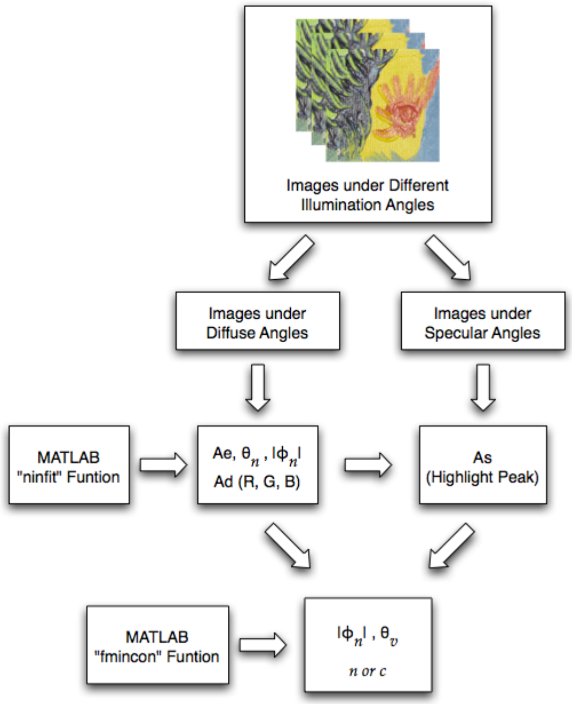

***Figure 3**. Diagram of flow for the estimation of the model parameters*

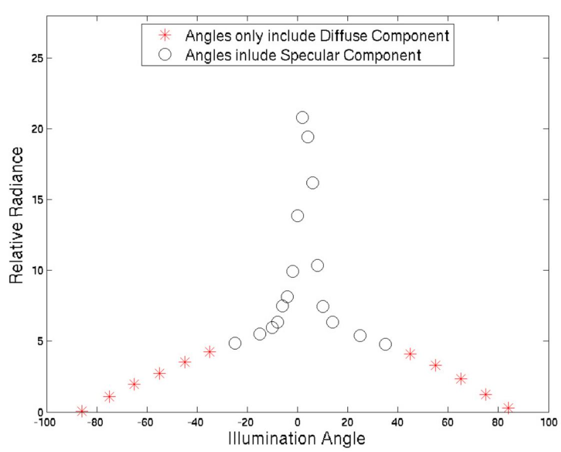

***Figure 4**. The separation of the diffuse and specular components*

Parameters Estimation for Specular Component

The magnitude values of the specular component should be fitted at first. With a collection of the highlight data, the pixel including the highlight peak was used to estimate the magnitude value. Therefore, for each pixel, θ_v, ϕ_v and n (or c) should be estimated finally. However, the sign of ϕ_n is unknown, which means it is impossible to estimate ϕ_v correctly. Since the tilt angles of the camera were very small, the alternative method is to estimate θ_v, n (or c) and empirical ϕ_n with the assumption that ϕ_v is equal to 0. The 'fmincon' non-linear optimization function was used in this step. The advantage of this function is that several variables can be optimized at one time.

Results and Discussions

In this research, eight artist paint samples were selected and measured to fit the two reflection models, as shown in Figure 5. Samples (a), (b) and (g) were painted on smooth surfaces. The varnished brush marks are shown on the sample (g), while samples (a) and (b) are almost uniform. Samples (c) and (d) were painted on uniform glass surfaces. Three canvas paint samples were also selected, as shown in samples (e), (f) and (h). In addition, these samples were selected from different gloss levels, as listed in Table I. The gloss values of different incident angles shown in the table were measure with a BYK Gardner glossmeter. The gloss levels of samples (e) – (h) were estimated based on the observation.

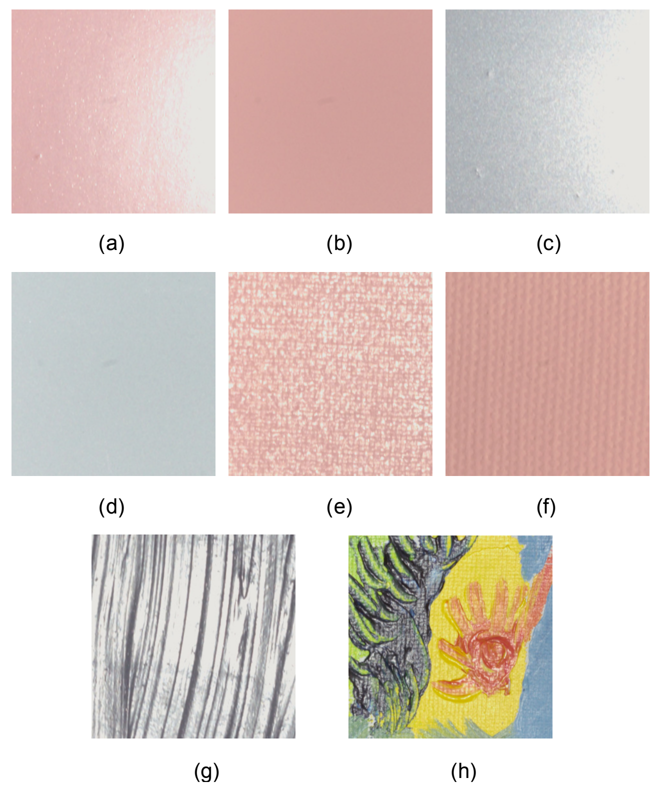

***Figure 5**. The eight paint samples used to fit two reflection models*

Table I. The gloss properties of the paint samples

	Gloss Levels	Gloss Values (85°)	Gloss Values (60°)	Gloss Values (20°)
(a)	High	83.5	66	24.3
(b)	Low	2.1	1.7	0.9
(c)	Medium	55.9	33.3	6.3
(d)	Low	4.5	2.5	0.5
(e)	Medium			
(f)	Low			
(g)	High			
(h)	Medium			

Physical-based Evaluation of Two Models

Based on the flowchart in Figure 3, the parameters of two models were estimated. The results of the estimation for the samples of three gloss levels are shown in Figures 6 – 8. It is obvious that the diffuse component can be estimated very well with the Gauss-Newton method. For the matte samples, such as sample (d), either the Phong or Torrance-Sparrow model could well estimate the specular component. With the increase in gloss, both models revealed worse fitting results for the specular component. However, the Torrance-Sparrow model had better fitting than the Phong model for the angles contained within the black ellipses shown in Figures 7 and 8. This indicates that the simple Phong model overpredicted the shininess of the sample. This result agrees with the experiment results of Tonsho.[12]

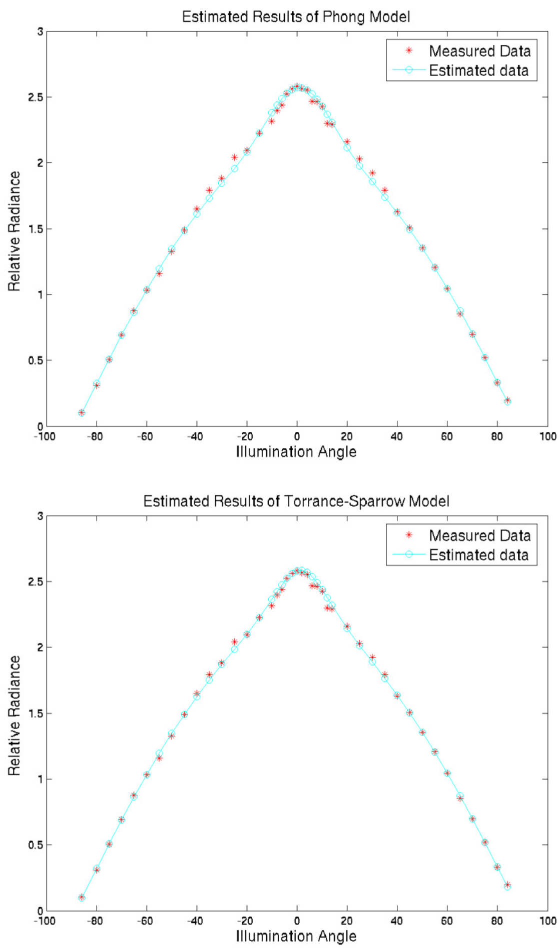

***Figure 6**. Estimation results of a pixel of sample (d)*

Furthermore, the estimated magnitude ratios of the specular components to the diffuse components are listed in Table II. Since there are several different paints on sample (h), the ratio of the sample is the average ratio of all the pixels. These ratios agree with the glossmeter values listed in Table I. The parameter n in Phong model and c in Torrance-Sparrow Model were estimated for each pixel in order to obtain optimized fitting.

Psychophysical Evaluation of Two Models

With the parameters of the two models, the estimated images under a series of different illumination angles can be rendered. To best reproduce the colors of the samples on the LCD monitor, the color management flow in Figure 9 was used.

To further evaluate the performance of two models, the paired-comparison psychophysical experiment was performed. The goal of this experiment was to determine the preferred model under certain illumination angles for each sample.

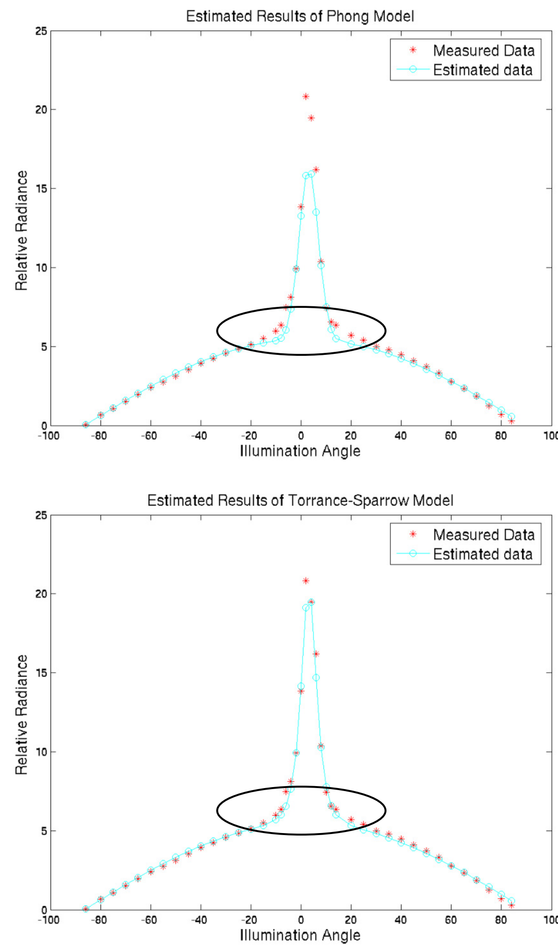

***Figure 7**. Estimation results of a pixel of sample (e)*

Table II. The estimated ratios of the specular component to the diffuse component

	Phong Model As/Ad	Torrance-Sparrow Model As/Ad
(a)	87.5	5793.6
(b)	0.2	3.8
(c)	23.8	1712.9
(d)	0.7	17.8
(e)	6.1	142.6
(f)	0.2	4.3
(g)	87.7	1752.1
(h)	11.9	560.9

The data from the experiment were analyzed using Thurston's Law of Comparative Judgments, Case V, and the evaluation results of eighteen observers are shown in Figure 10. In addition, the 95% confident limits were generated. The interval scales in Figure 10 illustrate the rendering accuracy of two models compared with the original photographs of the samples under all the test illumination angles, including the angles with and without specular component. For the samples with higher gloss levels, such as samples (a), (c), (e) and (g), Torrance-Sparrow model also produces higher visual accuracy, as well as the computational accuracy. For the matte samples (b), (d) and (f), two models provide similar rendering accuracy. Although sample (h) was estimated with medium gloss level, there is very little difference of the visual accuracies between two models. This indicates that the observers are difficult to notice the highlight differences of two estimated images for the sample with different materials, colors and complicated surface shape.

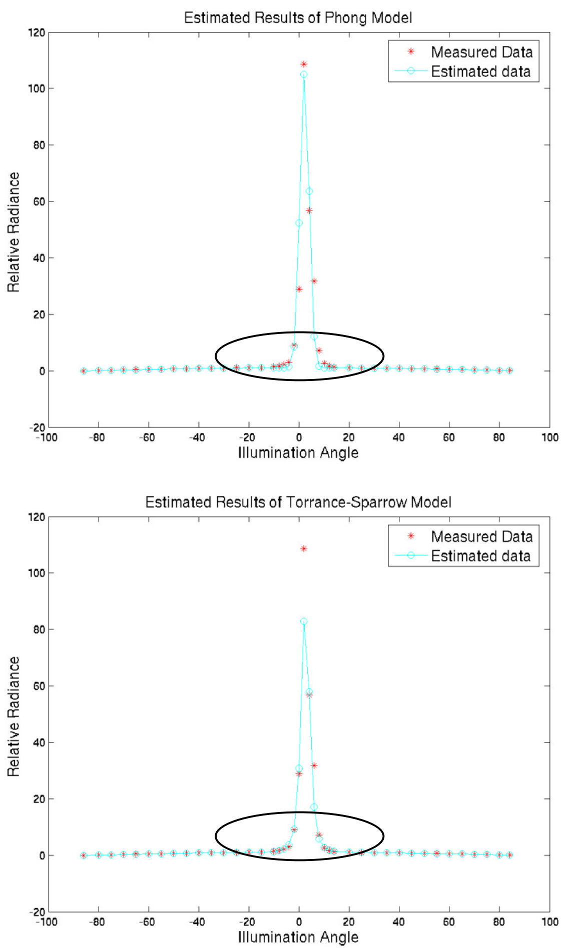

***Figure 8**. Estimation results of a pixel of sample (g)*

Minimization of the Number of Measurement

Since the Torrance-Sparrow model provides better overall prediction, it was used to minimize the angle number of measurement. Also, four of the eight samples with high and medium gloss levels were selected, which are samples (c), (e), (g) and (h). For each sample, there are five different groups of angle number selection. With each group, the parameters of Torrance-sparrow model were estimated. The paired-comparison experiment was also performed to evaluate the rendering accuracy optimized with different groups of angle number for seven illumination angles. In addition, the real images of the samples were used to detect if the reproduced images are significantly different with the real images.

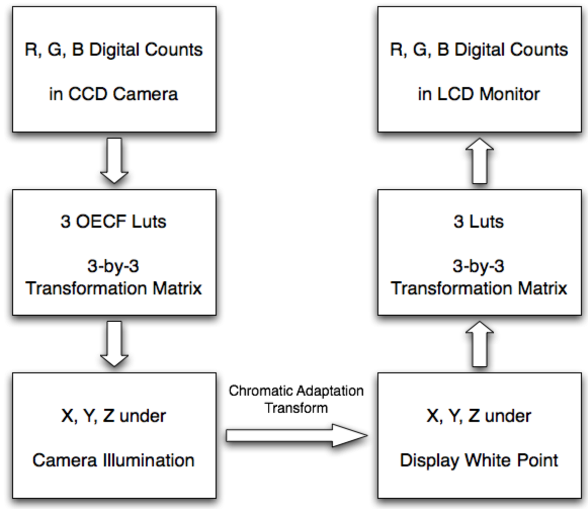

***Figure 9**. The flowchart of color management for image rendering*

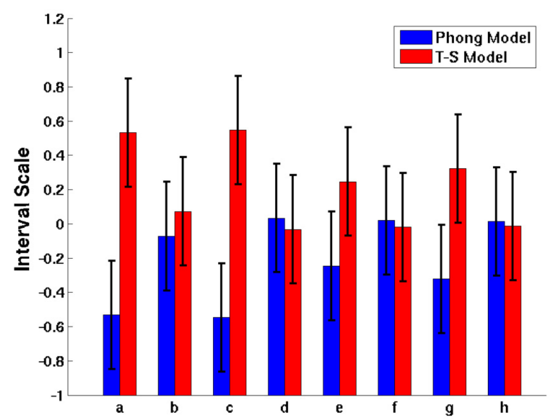

***Figure 10**. Interval scale of rendering accuracy of two models*

Sample (e) was taken as an example to show the results of the experiment in Figure 11. For the sample, it can found the rendering accuracy is high enough so that the observers cannot differentiate the real image from the reproduced images for all five groups of angle number. Correspondingly, RMS values of relative radiance of 20000 pixels for all illumination angles were calculated, as shown with blue points in Figure 12. To better improve the physical accuracy of the estimation with small amount of angle number, the angle positions should be carefully selected based on specular peak width and the histogram of the surface normal of all the pixels. Thus, for sample (e), the optimized group of angle number can be determined, which produces both rendering and physical accuracy, as shown in the red point in Figure 12. Therefore, this group of angle selection can be used for the paint samples with similar canvas surface and specular peak width values. Finally, the angle numbers of measurement of other three samples can also be determined, as shown in Table III.

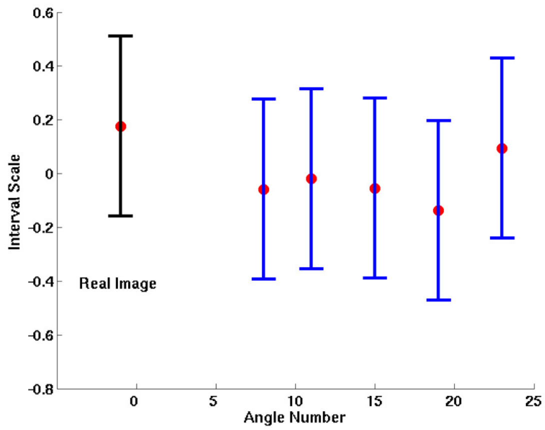

***Figure 11**. Interval scale of rendering accuracy optimized with different groups of angle number selection using Torrance-Sparrow Model for Sample (e)*

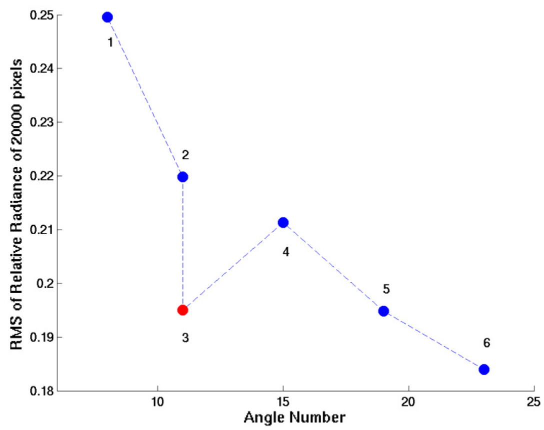

***Figure 12**. RMS values of the relative radiance of 2000 pixels optimized with different groups of angle number selection using Torrance-Sparrow Model for Sample (e)*

Table III. The minimized angle number for four samples

Sample	(c)	(e)	(g)	(h)
Minimized Angle Number	9	11	11	11

Conclusions

Two simple light reflection models, Phong and Torrance-Sparrow, were selected to estimate the gonio-radiometric properties of artist paint surfaces. A series of images under different illumination angles were captured to estimate the parameters of the model using MATLAB non-linear optimization functions. Eight paint samples with different textures and gloss levels were selected to evaluate the accuracy of two models. The evaluation results show that the diffuse components of all the samples can be estimated very well using both models. For the matte samples, the estimation accuracies of two models are almost the same. For the samples with higher gloss level, neither model produced perfect estimation, but the Torrance-Sparrow model showed better estimation accuracy than the Phong model. But for the samples with different materials and complex surface shape, two models provide similar visual accuracy. Furthermore, the minimized angle numbers of four different kinds of samples were determined with the analyses of their distribution of surface normal and the width of specular peak.

Reference

1. "Standard Practice for Angle Resolved Optical Scatter Measurement on Specular or Diffuse Surfaces", ASTM Standards E 1392-96, 1-12.
2. B. T. Phong, "Illumination for Computer Generated Pictures", Communications of the ACM, 311-317, 18, 1975.
3. G.J. Ward, "Measuring and Modeling Anisotropic Reflection", Computer Graphics, 265-272, July, 1992.
4. J.F. Blinn, "Models of Light Reflection for Computer Synthesized Pictures", In Proceedings of ACM SIGGRAPH'77, San Jose, 192-198, 1977.
5. K.E. Torrance, E.M. Sparrow, "Theory for Off-specular Reflection from Roughened Surfaces", Journal of Optical Society of America, 1105-1114, 57, 1967.
6. T.S. Trowbridge, K.P. Reitz, "Average irregularity representation of a rough surface for ray reflection", Journal of Optical Society of America, 531-536, May, 1975.
7. K.J. Dana, B. Ginneken, S.K. Nayar and J.J. Koenderink, "Reflectance and Texture of Real-World Surfaces", ACM Transactions on Graphics, 1-34, January 1999.
8. T. Malzbender, D. Gelb and H. Wolters, "Polynomial Texture Maps", The 28th Annual Conference on Computer Graphics and Interactive Techniques, 519-528, 2001.
9. T. Hawkins, J. Cohen and P. Debevec, "A Photometric Approach to Digitizing Cultural Artifacts", The 2001 Conference on Virtual Reality, Archeology, and Cultural Heritage, 333-342, November 2001.
10. S. Tominaga, T. Matsumoto and N. Tanaka, " 3D Recording and Rendering of Art Paintings", The 9th Color Imaging Conference, 337-341, 2001.
11. "ISO14524, Photography - Electronic still-picture cameras - Methods for measuring opto-electronic conversion functions (OECFs)", 1st Edition, 1999.
12. K. Tonsho, Y. Akao, N. Tsumura and Y, Miyake, "Development of Gonio-photometric Imaging System for Recording Reflectance Spectra of 3D Objects", Proceedings of SPIE, 370-378, 2002.

Author Biography

Ying Chen received her MS degree in Optical Engineering Department at Zhejiang University in China (2005). Now she is the master student in Munsell Color Science Laboratory at Rochester Institute of Technology. Her research mainly focuses on the evaluation of BRDF models for rendering art paintings and simplifying the gonio-spectrophotometer.